Global Maps of Mercury's Elemental Composition: New Results from Epithermal and Fast Neutrons. David J. Lawrence[1], William C. Feldman[2], Larry R. Nittler[3], Patrick N. Peplowski[1], Sean C. Solomon[3,4], Shoshana Z. Weider[3]; [1]Johns Hopkins University Applied Physics Laboratory, Laurel, MD 20723, USA (David.J.Lawrence@jhuapl.edu); [2]Planetary Science Institute, Tucson, AZ 85719, USA; [3]Carnegie Institution of Washington, Washington, DC 20015, USA; [4]Lamont-Doherty Earth Observatory, Columbia University, Palisades, NY 10964, USA

Introduction: A major objective of NASA's MErcury Surface, Space ENvironment, GEochemistry, and Ranging (MESSENGER) mission is to quantify and characterize Mercury's surface composition with the goal of improving our understanding of the planet's formation and geological history. To date, X-Ray Spectrometer (XRS) and Gamma-Ray Spectrometer (GRS) data have provided maps or hemispheric averages of the concentrations of K, Th, U, Na, Cl, and Si and ratios relative to Si of Mg, Al, S, Ca, Ti, and Fe [1–9]. Neutron Spectrometer (NS) measurements of Mercury's surface have also yielded estimates of polar H concentrations [10] and constraints on the abundance and spatial distribution of several elements (Fe, Ti, Cl, and Na) via measurements of thermal neutron absorption [11, 12].

These observations have revealed that in addition to water ice within permanently shadowed regions (PSRs) near Mercury's poles, Mercury's surface is globally richer in volatile elements (e.g., S, Na, K, Cl) than expected. In addition, these measurements have shown that Mercury's surface is compositionally heterogeneous and displays distinct geochemical terranes [9, 12]. However, there is much about Mercury's surface composition that is not well understood. Most importantly, many compositional boundaries do not coincide with boundaries defined on the basis of geological mapping or spectral reflectance [9, 12]. Moreover, knowledge of variations in composition is currently limited by coarse sampling resolution or a lack of coverage over large areas.

Here we report new surface compositional results for Mercury obtained from NS measurements of epithermal and fast neutrons. Compared with initial reports of regional polar variations [10], we now have five times more data, with much of those data acquired at lower average altitudes and hence better spatial resolution. These new data allow us to characterize the spatial heterogeneity of Mercury's polar hydrogen deposits and map the variations in average atomic mass across Mercury's northern hemisphere.

Planetary Neutron Spectroscopy: Planetary neutrons are created via nuclear spallation reactions when galactic cosmic rays impact a planet's surface. The energy-dependent neutron flux is naturally divided into three broad energy bands that characterize different aspects of a planet's surface composition. Thermal neutrons, which have a neutron kinetic energy, E_n, less than 0.4 eV, are sensitive to the presence of strongly neutron-absorbing elements such as Fe, Ti, Cl, Gd, and Sm. High-energy (E_n>0.5 MeV) fast neutrons are sensitive to the average atomic mass (<A>) of surface material and are also affected by H concentrations greater than a few hundred parts per million (ppm). Epithermal neutrons, which have energies between thermal and fast, are affected by the presence of H and are sensitive to concentrations as low as tens of ppm.

On the MESSENGER payload, thermal neutrons are measured both by the NS and by the anticoincidence shield that is part of MESSENGER's GRS. Epithermal and fast neutrons are measured with the NS. Global and regional measurements of thermal neutrons have been reported earlier [11, 12]. The initial reports of epithermal and fast neutrons used measurements acquired from the beginning of the orbital mission phase (18 March 2011) through February 2012. Here we report results taken with data from March 2011 through October 2014. These data represent a five-fold increase in near-planet accumulation due both to increased mission duration as well as the shorter 8-h orbits during the extended mission (since April 2012) compared with the 12-h orbits during the one-year primary mission. During MESSENGER's extended mission, the average altitude during periapsis passes has been reduced by more than a factor of two, which results in a proportional improvement in spatial resolution. This dataset therefore provides measurements with substantially enhanced statistical precision and spatial resolution and enables the construction of spatially resolved maps of epithermal and fast neutrons.

Epithermal Neutrons – Polar Count Rate Map: Prior measurements of epithermal neutron count rates showed a polar count rate decrease only within broad latitude bands. These data were shown to be consistent with the presence of large amounts of water ice within PSRs near the surface at high northern latitudes. Further, these results were consistent with other reflectance, topographic, and thermal modeling studies indicating the presence of water ice and other frozen volatiles within Mercury's polar deposits [13–15]. A new map of epithermal neutrons is shown in Fig. 1 along with the locations of radar-bright polar deposits, the expected sites of water ice at the surface. The measurements clearly show a count rate decrease indicative of enhanced hydrogen in locations similar to the polar deposits. These results confirm the earlier conclusion

that enhanced hydrogen concentrations in the form of water ice is the dominant compositional component of Mercury's polar deposits. The precise locations and signal magnitude of the measured count rates, however, are not identical to those from a simulation in which polar deposits consist of pure water ice extending to the surface. These data can therefore be used to test and quantify the horizontal extent and burial depth of Mercury's polar ice.

Fast Neutrons – Northern Hemisphere Map: A map of count rates for fast neutrons is shown in Fig. 2. This map shows clear compositional heterogeneities across Mercury's northern hemisphere that are consistent with prior measurements but also reveal new information. The fast neutron variations correlate with many prior mapped boundaries, including the exterior Caloris plains as well as extended portions of the northern plains. There is also a clear fast neutron enhancement co-located with the Mg-rich region identified from XRS data [9]. On the basis, in part, of prior studies, the simplest interpretation of this fast neutron map is that it provides a proxy for Fe variations across Mercury. Evidence for this interpretation includes enhanced Fe and neutron absorption in the high-Mg region and a region near (0°N, 60ºE), and relatively low Fe and neutron absorption in the Caloris basin and nearby regions. These regions show corresponding fast neutron enhancements and decreases, respectively. With the increased coverage provided by the fast neutron map, locations of low <A> (or low Fe) centered on (45ºN, 0°E) and high <A> (or high Fe) centered on (70°N, 120ºE) and (70ºN, 270°E) have been tentatively identified.

References: [1] Nittler, L.R. et al., *Science*, 333, 1847, 10.1126/science.1211567, 2011; [2] Peplowski, P. N. et al., *Science*, 333, 1850, 10.1126/science.1211576; [3] Peplowski, P.N. et al., *J. Geophys. Res.* 117, E00L04, 10.1029/1012JE004141, 2012; [4] Peplowski, P.N. et al., *Icarus*, 228, 86, 10.1016/j.icarus.2013.09.007, 2014; [5] Evans, L.G. et al., *J. Geophys. Res.*, 117, E00L07, 10.1029/2012JE004178, 2012; [6] Evans, L.G. et al., *LPS*, 45, 1794, 2014; [7] Weider, S.Z. et al., *J. Geophys. Res.*, 117, E00L05, 10.1029/2012JE004153, 2012; [8] Weider, S.Z. et al., *Icarus*, 235, 170, 10.1016/j.icarus.2013.03.002, 2014; [9] Weider, S.Z. et al., *Earth Planet. Sci. Lett.*, in review, 2015; [10] Lawrence, D.J. et al., *Science*, 229, 292, 10.1126/science.1229953, 2013; [11] Lawrence, D.J. et al., *Icarus*, 209, 195, 10.1016/j.icarus.2010.04.055, 2010; [12] Peplowski, P.N. et al., *Icarus*, in review, 2015; [13] Neumann, G.A. et al., *Science*, 229, 296, 10.1126/science.1229764, 2013; [14] Paige, D.A. et al., *Science*, 229, 300, 10.1126/science.1231106, 2013; [15] Chabot, N.L. et al., *Geology*, 42, 1051, 10.1130/G35916.1, 2014; [16] Denevi, B.W. et al., *J. Geophys. Res. Planets*, 118, 891, 10/1002.jgre.20075, 2013.

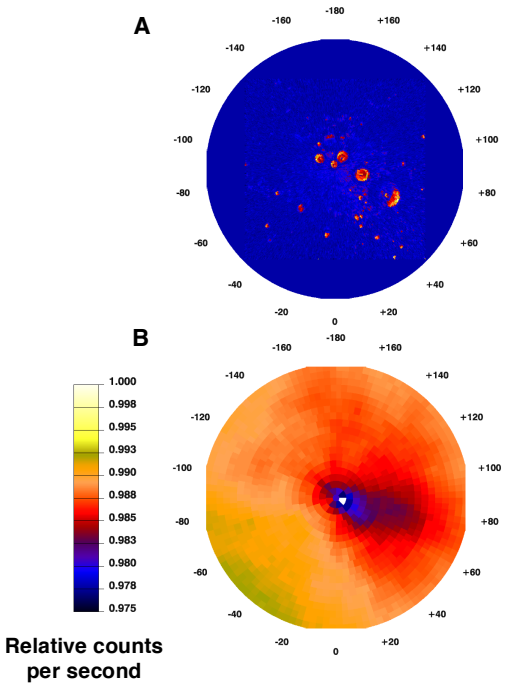

Fig. 1. Maps of Mercury poleward of 80ºN. (A) Locations of radar-bright polar deposits (red). (B) Epithermal neutron count rates relative to global mean count rate. Lower count rates indicate regions with enhanced hydrogen concentrations.

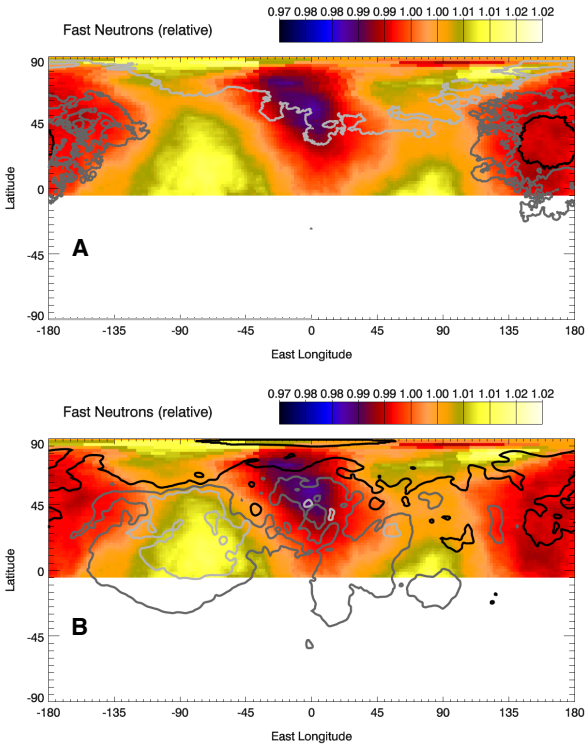

Fig. 2. Maps of fast neutron count rates relative to the global mean count rate. Available coverage is for regions poleward of ~0ºN. (A) Count rate map with boundaries of major smooth plains units [16]. (B) Count rate map with contours of Mg/Si ratio by weight. [7]. Contour values are 0.3 (black), 0.46 (dark grey), and 0.6 (light grey).